Estuarine, Coastal and Shelf Science 323 (2025) 109417

Contents lists available at ScienceDirect

Estuarine, Coastal and Shelf Science

journal homepage: www.elsevier.com/locate/ecss

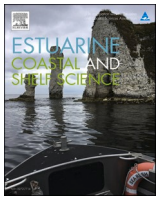

Erosion threshold of cohesive sediments in the German Wadden Sea: Temporal variability and comparison of in-situ and laboratory experiments

M. Witt [a,*], J. Patzke [a], E. Nehlsen [b], P. Fröhle [a]

[a] Institute for River and Coastal Engineering (IWB), Hamburg University of Technology, Hamburg, Germany
[b] Department of Architecture and Civil Engineering, Technical University of Applied Sciences Lübeck, Lübeck, Germany

ARTICLE INFO

Keywords:
Cohesive sediment
Erodibility
Erosion threshold
Mudflat
Wadden sea
Elbe
C-GEMS

ABSTRACT

A newly developed in-situ setup of the Closed Gust Erosion Microcosm System (C-GEMS) was utilized for erosion experiments in a tidal mudflat in the mouth of the Elbe in the German Wadden Sea to investigate the temporal variability of the erosion threshold τ_c of cohesive sediments. In addition, erosion experiments with extracted sediment cores from the same site were conducted in the field and in the laboratory with the identical device to analyze the influence of sample extraction and transport on the derived erosion threshold. A total of 21 erosion experiments were carried out in four measuring campaigns between April and September 2024. The erosion thresholds derived from the in-situ experiments exhibit considerable temporal variability across campaigns, with values of τ_c = 0.1–0.27 N/m^2, while repeated experiments within the individual campaigns demonstrate a high degree of reproducibility. Accompanying analyses of surface sediment particle size distribution and bulk density revealed that mud concentration (clay and silt) varied with wind conditions and the associated hydrodynamic load prior to the measurement campaigns. The observed temporal variability in τ_c is reasonably well captured by a mathematical model based on mud concentration and particle size, suggesting that τ_c can be plausibly estimated from these parameters. For campaigns with a cohesive surface sediment layer, erosion thresholds derived in the ex-situ experiments are consistently lower than those obtained in the in-situ experiments. This is attributed to the disturbance of the surface sediments due to mechanical extraction and liquefaction during transport. The findings offer insights into the transport dynamics of cohesive sediments and help guide decisions on whether future erosion experiments should be conducted in situ, despite the significant effort involved, or whether extracted sediment cores are a suitable alternative.

1. Introduction

Intertidal mudflats cover large areas of estuaries and sheltered coastal zones and may act as both a sink or source of cohesive sediments. To improve the understanding of the exchange processes between mudflats and adjacent estuarine and coastal waters, characterizing the erosion behavior of cohesive sediments is essential. While the erosion of non-cohesive sediments is dominated by the particles size and shape of the sediment particles (Shields, 1936), the erodibility (erosion threshold and rate) of cohesive sediments is further influenced by a variety of physical, biological and geochemical parameters and therefore still difficult to predict (Berlamont et al., 1993; Grabowski et al., 2011). The cohesive or non-cohesive behavior of a sediment mixture is primarily influenced by the content of very fine sediments (clay and fine silt), as cohesion increases with decreasing particle size (Mehta and McAnally, 2008; Ternat et al., 2008). A clay content of 5–10 % is often reported as the threshold for cohesive behavior of sediment mixtures (van Rijn, 1993; Winterwerp et al., 2021). The erosion threshold of a sediment mixture generally increases with an increasing mud fraction (clay and silt), reaching its maximum at a mud fraction of 30–40 % (Panagiotopoulos et al., 1997; Ternat et al., 2008; Perkey et al., 2020). Debnath and Chaudhuri (2010) provide an overview of various definitions of the erosion threshold and summarize values obtained from field and laboratory experiments. Erosion thresholds are commonly estimated based on the bulk density or water content (Amos et al., 1997; Aberle et al., 2004), the mud content (Mitchener and Torfs, 1996) or, as a combination of the forementioned parameters, on the dry bulk density of the mud component (Chen et al., 2021) of a cohesive sediment mixture. In mudflats, microphytobenthos and macrozoobenthos have been observed to influence the erosion threshold as well (Widdows et al.,

* Corresponding author.
E-mail address: markus.witt@tuhh.de (M. Witt).

https://doi.org/10.1016/j.ecss.2025.109417
Received 29 January 2025; Received in revised form 18 June 2025; Accepted 25 June 2025
Available online 25 June 2025

2000; Andersen et al., 2010). Microphytobenthos is associated with an increasing erosion threshold (biostabilisation) and macrozoobenthos with a decreasing erosion threshold (bioturbation). Several studies have shown that the erodibility of intertidal mudflats can vary considerably in space and time (Houwing, 1999; Andersen, 2001; Zhu et al., 2019). This variability underscores the need for detailed field studies to better constrain and predict erosion dynamics in these environments.

The Wadden Sea is the world's largest interconnected system of sand and mudflats and has been at the center of competing demands such as navigation, flood protection and nature conservation for centuries (Lotze et al., 2005). While the Wadden Sea is largely dominated by sandy surface sediments, fine, cohesive sediments tend to accumulate particularly in nearshore areas (Sievers et al., 2021). Recent large-scale studies based on long-term bathymetry and surface sediment composition data, revealed two phenomena: First, a gradual increase of mudflats in the German Wadden Sea (Lepper, 2023), with potentially negative impacts on e.g. tourism and shipping, and second, that the mud-budget of the Wadden Sea as a whole is nearly closed, indicating that mud has to be treated as a finite resource (Colina Alonso et al., 2024). Additionally, during the 2010s, German authorities observed a significant increase in suspended sediment concentration (SSC) and deposition of fine sediments in the inner Elbe estuary, leading to an increase in maintenance dredging, especially in the area of the Port of Hamburg, and therefore financial and ecological burdens (Weilbeer et al., 2021). One major driver of this development is seen in the re-mobilization of fine sediments from tidal mudflats in the river mouth during two consecutive storm surges at the end of 2013, followed by upstream transport into the estuary under flood-dominated tidal conditions. To improve the understanding of the described developments and interrelations for past as well as future scenarios and to work towards a sustainable sediment management, large-scale hydro- and morphodynamic numerical models are increasingly applied, which need to be calibrated and validated based on reliable field data.

Erosion experiments with natural cohesive sediment samples can be conducted either directly in-situ on the sediment bed or ex-situ with extracted sediment samples, either at the sampling site or in laboratory. Because the extraction and transport of cohesive sediment samples may disturb the sediment structure, several authors recommend the in-situ determination of erosion characteristics (Berlamont et al., 1993; Whitehouse et al., 2000). However, in-situ measurements typically involve considerably more effort than ex-situ experiments. Over the past decades, a range of erosion devices has been developed, most of which are designed for one specific type of experiment (in-situ, ex-situ with extracted-cores or ex-situ with artificially placed beds). The in-situ devices in particular are often large and difficult to handle. Summaries of the existing devices can be found in Lee and Mehta (1994), Widdows et al. (2007) and Beckers (2021). Several studies have shown that the utilized device, measuring technique and the experimental procedure may significantly affect the erosion parameters obtained (Tolhurst et al., 2000a; Widdows et al., 2007).

To date, only a limited number of studies have addressed the potential influence of the extraction and transport of sediment samples on the derived erosions parameters in detail. Importantly, previous studies have generally involved different erosion devices for the in-situ and ex-situ experiments, making it difficult to isolate the effects of sample handling. Noack et al. (2015) investigated the erosion thresholds of cohesive sediments from the middle course of the Elbe and Saale Rivers both in-situ and in the laboratory. For the in-situ measurements, a benthic flow-through flume was placed onto the river bed, whereas for the laboratory experiments a different flume was used, in which previously extracted sediment cores were incrementally inserted from the bottom of the flume. Differences in flume dimensions and instrumentation limit the comparability of the results. The authors reported increases in mean τ_c of 20 % (Elbe) and 44 % (Saale) in laboratory experiments, attributing the differences to disturbances or loss of the fluffy top layer of the sediment during withdrawal and transport of the sediment cores. Tolhurst et al. (2000b) compared the results for τ_c from in-situ measurements with an annular flume with laboratory experiments in a straight flume for sediments from mudflats in the Humber estuary. The values for τ_c derived from the laboratory experiments were significantly higher than the in-situ measurements (lab.: 1.7–8 N/m^2; in-situ: 0.01–0.58 N/m^2). The authors attributed this discrepancy to the drying and compaction of the surface sediments during the transport of the sediment samples, as the samples were transported in a dry state, i.e., without a water column above the sediment surface. In the same study, results from in-situ measurements with a cohesive strength meter (CSM) in the Sylt-Rømø Bight were compared to laboratory experiments with an EROMES device (see Tolhurst et al. (2000b)) for a description of both devices). In this case, the samples for the laboratory experiments were transported with a 30 cm water column above the sediment surface. The results exhibited large scatter, yet after a recalibration of the EROMES results based on the CSM results, the authors concluded that the influence of the sampling and transport on τ_c may be rather small compared to other factors, if conducted carefully.

To address the described challenges, the present study aims to improve the understanding of the variability of the erosion threshold of cohesive sediments and to form a basis for future numerical and experimental investigations. The specific objectives can be summarized as follows.

- Development and presentation of a microcosm setup suitable for both in-situ erosion experiments and experiments with extracted sediment cores.
- Execution and evaluation of in-situ measurements of τ_c in an intertidal mudflat in the German Wadden Sea under varying environmental conditions and accompanying investigation of the changes in composition and concentration of the surface sediments.
- Comparison of the in-situ measurements of τ_c with ex-situ experiments conducted immediately after sample extraction on site and after transport to the laboratory, using the same erosion device and experimental procedure.

2. Study site and measuring campaigns

2.1. Overview

Four measurement campaigns were carried out between April and September 2024 at the location "Trischendamm" in the German Wadden Sea (Fig. 1). Each campaign consisted of two consecutive days of field measurements and sampling, followed by additional laboratory experiments. On each day in the field, both one in-situ erosion experiment and and one ex-situ (field) experiment with an extracted sample were performed (TD1 only in-situ). In addition, on each field day one sediment sample was collected for the ex-situ (lab.) experiments, which were conducted ~48 h after sampling. For TD3, one in-situ erosion experiment had to be excluded due to problems with the measuring devices, so a total of 21 erosion experiments were conducted, of which 7 were conducted in-situ, 6 ex-situ at site in the field and 8 ex-situ in the laboratory (see Table 1).

To characterize the sediment properties of the upper sediment layers of the mudflat, subsamples were taken at continuous depths of up to ~12 cm below the sediment surface during each campaign. The derived sediment properties are used to investigate the temporal variability of the depth-resolved sediment composition and concentration in the upper mudflat layers between the campaigns.

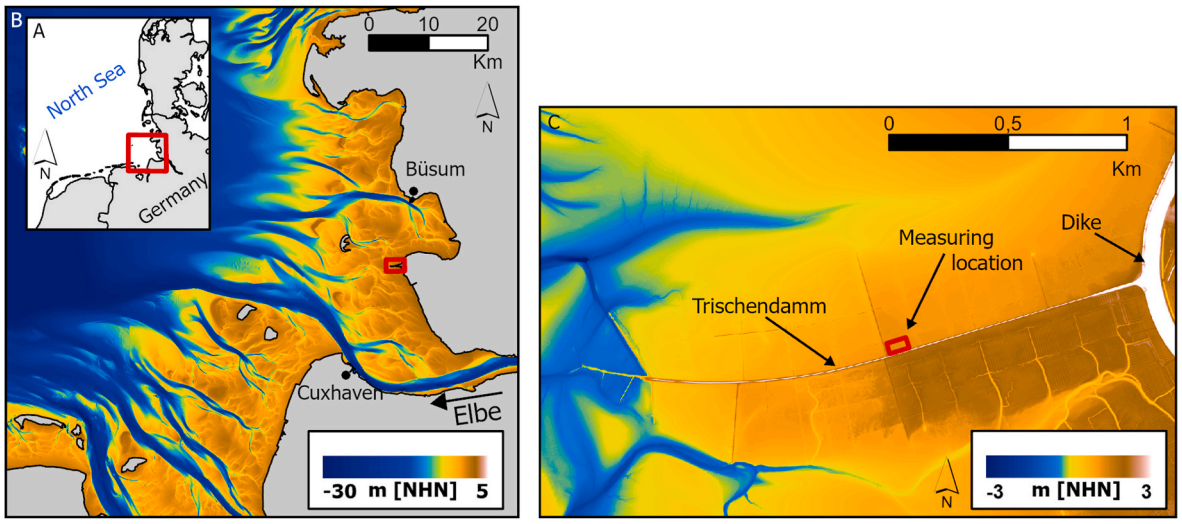

Fig. 1. Measuring and sampling location on the northern side of the "Trischendamm" in the outer Elbe estuary (data: DEM10-2022 (Panel B): BAW (2024); DEM1-2022 (Panel C): WSV (2024a)).

Table 1
Overview of the conducted measurement campaigns and experiments. Ex-situ (field) experiments were initiated in response to TD1 results from campaign TD2 onwards, to distinguish the effects of sample extraction and transport on the erosion threshold.

Campaign	Date	Erosion experiments			Subsamples for sed. charac.
		In-situ	Ex-situ (field)	Ex-situ (lab.)	
TD1	16.+17/04/24	2	–	2	x
TD2	14.+15/05/24	2	2	2	x
TD3	27.+28/08/24	1	2	2	x
TD4	24.+25/09/24	2	2	2	x

2.2. Location

The four measurement campaigns were carried out at the same location in an intertidal mudflat of the outer Elbe estuary in the German Wadden Sea (Fig. 1). The mudflat on the northern side of the "Trischendamm" was chosen based on three main criteria: i) a sediment composition dominated by fine sediments (clay and silt), ii) a sufficiently long exposure period during the low water phase, allowing for the in-situ erosion experiments to be carried out and iii) the accessibility, under consideration of the required measurement equipment and the minimization of the disturbance during transport of the sediment samples taken for the laboratory experiments.

The "Trischendamm" is an approximately 2.2 km long cross-shore structure, built to secure the dike line of the peninsula "Friedrichskoog" (Lorenzen, 1960). On both sides of the dam, groynes extend perpendicular to the dam into the mudflats. In some parts, remains of rectangular systems of brushwood fences exist, which were installed to increase sedimentation in this area. Over the past decades, salt marshes have developed on the southern side of the dam. As the dam crest is at +3.0 m NHN and the mean high-water level is approx. MHW = +1.61 m NHN (Büsum gauge), the dam is rarely overtopped.

The erosion experiments and the extraction of sediment samples were conducted halfway along the dam in a distance of ~20 m to the dam (see Fig. 1C). The experiments and samples of all campaigns were conducted or taken within a maximum distance of ~30 m from each other, with attention paid to the visual comparability of the sediment surface between the different experiments of a campaign. The altitude of the mudflat in the designated measuring area was determined as +1.22 m NHN in May 2024 by RTK-corrected GNSS measurement. The tide is semi-diurnal, with a mean-tidal range of MTR = 3.2 m and is therefore classified as mesotidal. Due to the altitude of the measuring location in relation to the mean high and low tides, the location is part of the high intertidal zone, which offers relatively short inundation times (see Fig. 2A–B). Between January and September 2024, the measuring location was inundated for 28 % of the time.

2.3. Environmental conditions during the measurement campaigns

The measuring campaigns were conducted during neap periods, to ensure sufficient time for the in-situ erosion experiments. During neap tides, the experimental area might not get inundated during single high tides (see Fig. 2A–B), which was the case for the high tide in the early morning before the measurements on 17/04/24 and 15/05/24 (day two of TD1 and TD2, respectively). Since in both cases the area was inundated during the previous evening high tide, the area was exposed to very little evaporation due to the absence of relevant solar radiation and was still covered by a film of water at the chosen sampling locations when starting the experiments in the morning, the effect of air exposure time on the erosion characteristics of the sediments is seen to be negligible.

Wind data measured at the weather station Büsum (Deutscher Wetterdienst, 2024) show comparable wind conditions for the period before campaigns TD1 and TD3 (Fig. 2C–D). During the week before each of the two campaigns, strong to stormy winds from southwestern directions dominated, leading to a leeward position of the measuring area in relation to the dam and therefore rather calm water conditions with no significant waves. In the days directly preceding and during TD2, fresh to strong winds from eastern directions occurred, and also around 01/05/24, two weeks before TD2, a distinct wind event with winds from the northeast took place. Under these wind conditions, the measuring area is more exposed to wind waves (H_s ~ 0.1–0.2 m). Before campaign TD4, trends in the wind conditions were less pronounced. In the week preceding TD4, weak to moderate winds from northeast dominated, turning to southwest during the campaign.

During campaigns TD3 and TD4, the surface of the mudflat within the designated measuring area was covered by a thin biofilm, the occurrence of which seems to be favored by high temperatures and solar radiation. The biofilm might have an influence on the erodibility of the sediment (see section 1), but no further measurements to characterize the biofilm were conducted, since this is out of the scope of the present study.

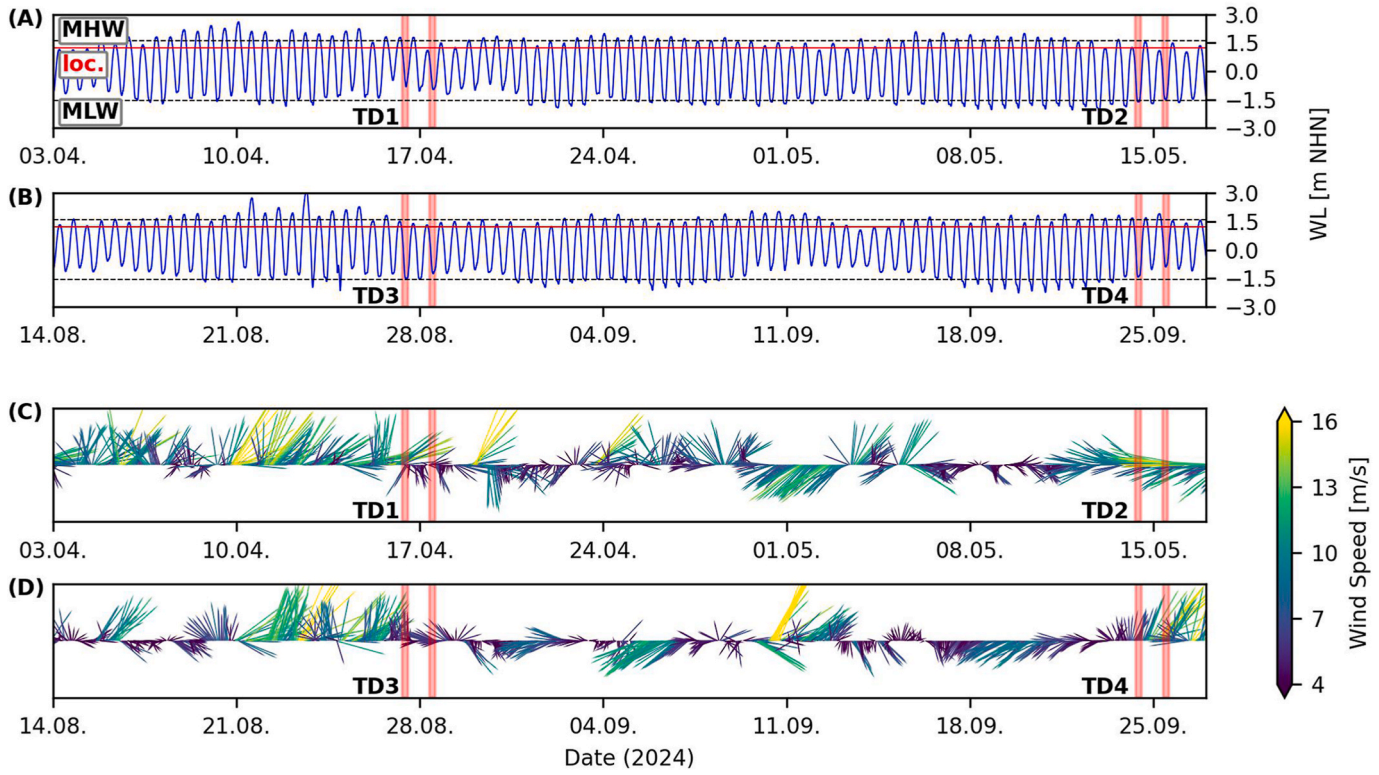

Fig. 2. Panels A–B show the water level measured at the gauge "Büsum" (data: WSV (2024b)) in relation to the elevation of the measuring location (MHW=+1.61 m; MLW=−1.56 m). Panels C–D show the wind speed and direction measured at the weather station "Büsum" (e.g., arrow to the top indicates wind from south; data: Deutscher Wetterdienst (2024), averaged per hour). In all panels the periods of the in-situ measurements are marked in red. (For interpretation of the references to colour in this figure legend, the reader is referred to the Web version of this article.)

3. Material and methods

3.1. Erosion experiments

3.1.1. Closed Gust Erosion Microcosm System (C-GEMS)

A Closed Gust Erosion Microcosm System (C-GEMS), introduced in Patzke et al. (2022) and described in detail in Witt et al. (2024), was utilized for the erosion experiments in this study. In the mentioned studies, the C-GEMS was used for erosion experiments with extracted sediment cores from a navigation channel (Patzke et al., 2022) and with placed beds in the laboratory (Witt et al., 2024). In this study, an extended in-situ setup of the device is introduced.

The original version of the GEMS was presented by Gust (1989), as an apparatus to apply precisely defined bed shear stresses to a sediment surface. It consists of a cylindrical housing, herein called erosion chamber, which contains the sediment sample in the lower part and water in the section above. A stirring disk, positioned at a defined distance from the sediment surface, induces a rotational flow. Water is pumped from the erosion chamber through the center of the stirring disk and replaced via an eccentric inlet in the chamber's lid at the same rate. The applied bed shear stress depends on both the rotational speed of the stirring disk (N) and the pumping rate (Q) (Gust, 1989; Gust and Müller, 1997). Measuring the suspended sediment concentration (SSC) within the effluent from the erosion chamber allows for the derivation of the temporal evolution of the erosion process over the experimental duration.

The GEMS is a widely used device to determine the erosion characteristics of cohesive sediment beds and is generally deployed as i) an open system and ii) with sediment cores, which were extracted in the field and subsequently installed into the device (Dickhudt et al., 2011; Briggs et al., 2015; Work and Schoellhamer, 2018; Seo et al., 2020; Ha and Ha, 2021). The term "open system" of the GEMS refers to the water pumped from the erosion chamber, which is continuously replaced by clear water from a reservoir. Accordingly, the suspended sediment concentration (SSC) does not accumulate in the system over the duration of the experiment.

In contrast to the GEMS, the C-GEMS is a closed system, in which the effluent from the erosion chamber is pumped to a second chamber, the measuring chamber, from which it is recirculated to the erosion chamber at the same rate. Thus, the system is closed and suspended sediments accumulate over the experimental duration. In the measuring chamber, the SSC is continuously measured throughout the duration of the experiment. A circulation pump prevents settling of the sediment particles and ensures a homogeneous distribution of the SSC in the measuring chamber. The SSC measurement is conducted by a highly sensitive Hach® Solitax hs-line sc probe, which operates on a combined infrared absorption scattered light technique and checked by density measurements with an Anton Paar DMA 35. The inner diameter of the erosion chamber (or sample cylinders) of the utilized C-GEMS is 20 cm and the stirring disk is adjusted in a distance of 7 cm to the sediment surface. The functional relationship between τ_b, Q and N can be found in Witt et al. (2024). A major advantage of the C-GEMS is the low consumption of processing water, which facilitates the mobile application of the device. In this study, the C-GEMS was deployed for direct in-situ erosion experiments for the first time. For the in-situ measurements, the C-GEMS was mounted onto a piercing cylinder, which was inserted into the mudflat (see section 3.1.3). Additionally, the device was equipped with a mobile battery pack for all experiments conducted in the field.

3.1.2. Experimental procedure and data processing

During the erosion experiments, the applied bed shear stress was increased stepwise from 0.03 to 0.34 N/m^2 across 13 load steps. Each load step had a duration of 15 min, leading to a total experimental

duration of 3.25 h.

The SSC was measured by the Hach® Solitax hs-line sc probe at a frequency of 0.2 Hz. To reduce scatter in the data, a moving average over 60 s was applied to the raw data before further processing. The measured SSC data were corrected by the initial SSC of the site-specific water used for the experiments, thus the increase in SSC in relation to the initial concentration was captured. Over the entire duration of the in-situ experiments, between 0.2 and 0.5 L of water were lost due to percolation, representing max. ~5 % of the system's total fluid volume. As the percolation rate was fairly constant throughout the experiments, a steadily decreasing fluid volume over the experimental duration was assumed for the calculations. The SSC values measured in the in-situ experiments were projected to the nominal total fluid volume accordingly. Since the loss of water during the in-situ experiments conducted in this study was comparatively small, the effect of the applied correction is marginal. However, when working with more permeable sediment layers, it might become relevant. The erosion rates ε [kg/(m^{2}s)] were calculated from the change in SSC between two consecutive time steps, taking into account the fluid volume of the system and the sediment surface area.

The applied method to derive the critical erosion threshold τ_c from the SSC-data was presented and validated in Witt et al. (2024). The method is based on a log-log regression between the mean SSC per load step and the applied bed shear stress τ_b (Eq. (1)):

$$\boldsymbol{ln(SSC) = m^{*} ln(\tau_b) + a} \quad \text{Eq. 1}$$

Herein, m and a denote the regression parameters. The critical bed shear stress τ_c is determined as the interpolated value where the regression line intersects the natural logarithm of the SSC threshold (SSC_T = 40 mg/l). This value represents the surface erosion threshold, hence minor erosion may occur below this value due to floc erosion (Winterwerp et al., 2021). Log-log regression provides equal weighting to values across different orders of magnitude. The resulting relationship can be transformed back into linear space as $SSC = e^{a}\tau_b^{m}$, representing a power-law relationship between SSC and τ_b. A key advantage of this method is its high level of automation, which reduces subjective data interpretation in the derivation of τ_c. In this study, this method was applied with a slight modification: load steps with a mean SSC below 2 mg/l were excluded to enhance the stability of the method.

3.1.3. Sample preparation, extraction and transport

For the in-situ experiments, an acrylic piercing cylinder with a diameter of 20 cm was inserted directly into the mudflat to a depth of approx. 20–25 cm. Site specific water, which was collected during high tide for each measuring campaign, was added to the cylinder above the sediment surface (ρ_w ~ 1018 kg/m^3; salinity: 20–25 PSU). This process was conducted very carefully (~15 min for 3 L of water), ensuring minimal disturbance and no measurable resuspension of the surface sediments. After mounting the C-GEMS onto the piercing cylinder, the lid and the stirring disk were carefully lowered to the intended distance from the sediment surface (Fig. 3A). The supplementary devices needed (namely a battery pack, the measuring chamber, controllers for both the C-GEMS and the Solitax SSC probe), were transported to the measuring location using a mud sledge.

For the ex-situ (field) experiments conducted in the vicinity of the measuring site and the ex-situ (lab.) experiments, mostly undisturbed sediment samples were extracted from the mudflat. Cylinders of equivalent diameter to those used in the in-situ experiments were inserted to the sediment and sealed with an airtight top-plug. After the sediment around the cylinder had been removed, the samples could be easily extracted due to the sticky nature of the sediment and the under-pressure in the cylinder. Directly after the extraction, another air- and watertight plug was inserted at the bottom of the cylinder (with pressure compensation through the top-plug). After removing the top-plug again, site-specific water was added on top of the sediment surface, as previously described for the in-situ experiments. The samples prepared in this way were either directly installed into the sample holder for the ex-situ (field) experiments (Fig. 3B) or sealed again for the transport to the laboratory. The ex-situ (field) experiments were initiated approximately 2 h after extraction of the sediment samples.

The transportation of the sediment samples to the laboratory was conducted by a handcart on the Trischendamm and subsequently by car. For campaign TD1, a handcart with hard rubber tires was used, which, in combination with the rough and partially damaged asphalt surface of the Trischendamm, led to a vibration exposure of the sediment samples. For all following campaigns, a handcart with large pneumatic tires was used to minimize vibrations during transport. The ex-situ erosion experiments in the laboratory were carried out approximately 48 h after extraction of the respective sediment sample. The time span of 48 h was chosen to ensure uniform test conditions for the samples collected on the two consecutive field days of each campaign and yet limit possible

Fig. 3. A) In-situ erosion experiment in a tidal mudflat with the C-GEMS. B) Ex-situ (field) experiment with an extracted sediment core directly at the sampling site. Measuring chamber, controllers and battery pack are stored on a mud sledge outside pictures A and B. C-D) Surface of the mudflat during TD1 (C) and TD2 (D). The hole in each of the latter pictures has a diameter of 20 cm.

temporal effects on the erosion characteristics.

To collect the sediment samples used for the characterization of the depth-resolved sediment properties, another cylinder was inserted to the mudflat and the sediment inside the cylinder was carefully extracted and filled into separate containers in layers of generally 2–3 cm. During campaigns TD1, TD2 and TD4 a distinct layer of 1–2 cm of soft freshly deposited material was present at the sediment surface, which clearly differed from the denser layers below (Fig. 3C). To capture the properties of this layer separately, the topmost sample included only this section of 1–2 cm for the respective campaigns. During the TD2 campaign, no such distinct layer was present and the topmost 0.5 cm were taken as separate sample to characterize the surface sediments (Fig. 3D).

3.2. Characterization of sediment properties

The particle size distributions (PSD) of the sediment samples were determined by a combined sieve and hydrometer analysis following ISO 17982-4 (DIN, 2017). The water content (W) was determined by oven drying at 105 °C after ISO 17982-1 (DIN, 2022) and is expressed in relation to the weight of the solid matter of the sample. The loss on ignition (LOI) was determined after EN 17685-1 (DIN, 2023) by annealing at 550 °C as a proxy for the organic content of the samples. The bulk density (ρ_b) of the sediment samples was measured using a suspension balance and checked by measurements with an Anton Paar DMA 35 density meter for densities below ~1400 kg/m^3.

4. Results and discussion

4.1. Sediment characteristics

As outlined in section 3.1.3, subsamples of the mudflat sediments were collected up to a depth of ~12.5 cm below the sediment surface during each measuring campaign. These subsamples were used to derive depth-dependent sediment properties. Fig. 4A illustrates the results for the water content and Fig. 4B for the bulk density. Focusing on the water content in Fig. 4A, it is evident, that the water content near the sediment surface varied significantly for the different measuring campaigns. While for TD2, the water content of the topmost sediment layer was ~95 %, it was ~280 % at the time of TD3. The obtained water content of the TD1 and TD4 surface layers was in the range between these minimum and maximum values. Over the upper 5 cm, a sharp decrease in water content was observed for all measuring campaigns, reaching a uniform lower bound of ~50 %. The depth, in which this equilibrium water content was reached and the water content in the transition area depended on the water content of the mudflat's surface sediments. Since a high water content of a sample implies a low sediment concentration and therefore a low bulk density, the depth-dependent bulk densities illustrated in Fig. 4B show the opposite trends compared to the depth-dependent water contents. The bulk densities of the surface layer ranged between 1200 kg/m^3 (TD3) and 1460 kg/m^3 (TD2) and reached a bulk density of ~1600 kg/m^3 in a depth of 5–10 cm. The LOI of the surface layer ranged from 8 % to 13 % across the campaigns (TD1: 12 %, TD2: 10 %, TD3: 13 %, TD4: 8 %). In the layers below, LOI values ranged from 4 % to 9 % in all campaigns, showing a general trend of decreasing LOI with increasing depth.

In addition to water content, bulk density and LOI, the PSD of the upper sediment layers was analyzed. Fig. 5 presents the results for all measurement campaigns, covering depths of up to 10 cm below the sediment surface. The topmost subsample represented the layer of soft, freshly deposited sediment (1–2 cm thick) when present, as in campaigns TD1, TD3, and TD4. For TD2, where no such fresh layer was found, the uppermost 0.5 cm was sampled to characterize the surface sediments. Similar to water content and bulk density, the surface layer

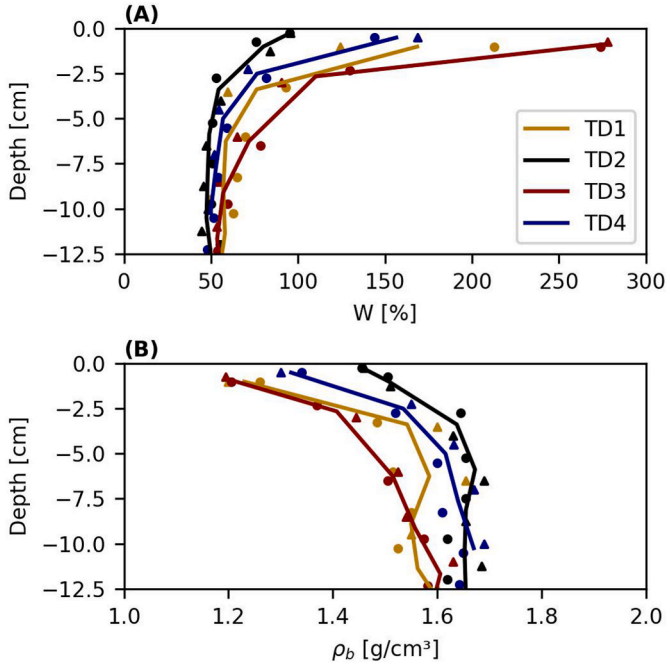

Fig. 4. Water content (A) and bulk density (B) of the upper sediment layers at the time of the respective measuring campaign. Two sets of subsmaples were collected for each campaign (indicated by triangle/circle). The drawn lines show the interpolated depth and water content/bulk density for the corresponding subsamples.

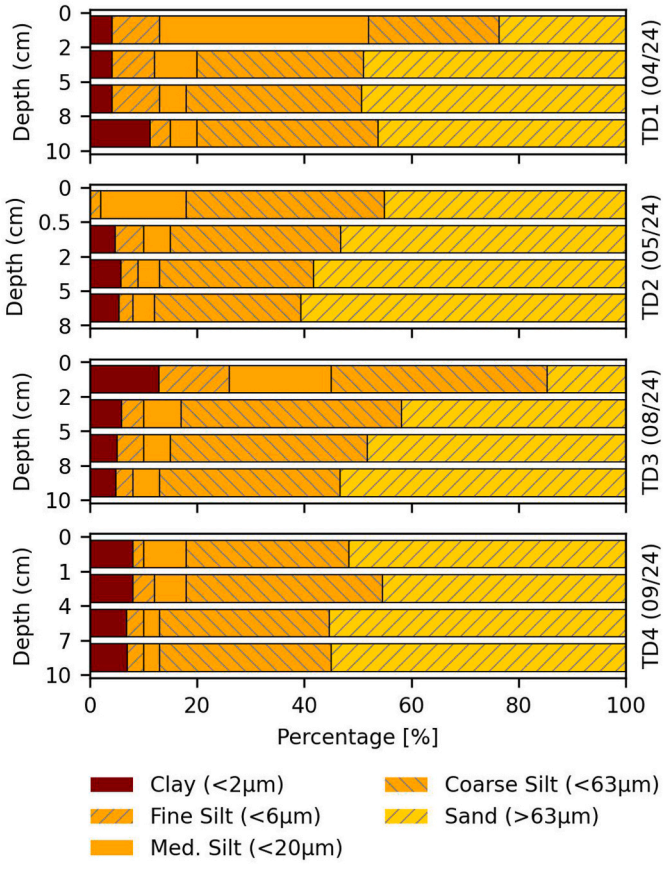

Fig. 5. Depth-dependent PSD for the upper sediment layers at the time of the respective measuring campaign. The topmost subsample (surface sediments) included only the soft layer of freshly deposited sediments for campaigns TD1, TD3 and TD4. During TD2, no layer of freshly deposited material was present.

PSD varied considerably. Fine sediment content (clay and silt) ranged from ~80 to 90 % in TD1 and TD3, but only ~50–60 % in TD2 and TD4. In contrast, the deeper layers showed consistent PSD profiles across all campaigns, with no significant changes with depth.

As mentioned in section 1, the cohesive or non-cohesive behavior of a sediment mixture is primarily determined by the content of very fine particles (clay and fine silt) and a clay fraction of just 5–10 % is sufficient to induce cohesive behavior. In the surface layer, the clay and fine silt fraction ranged from 10 % to 26 % in TD1, TD3 and TD4, indicating cohesive sediment mixtures. In contrast, the surface layer in TD2 contained no clay and only negligible amounts of fine silt, suggesting non-cohesive or only weakly cohesive behavior. The differences in the water content and PSD of the surface sediments were likely caused by the wind conditions and the resulting hydrodynamic loading of the sediment surface in the period prior to each measuring campaign (see section 2.3). Campaigns TD1 and TD3 were preceded by periods of strong south-westerly winds, but rather calm water conditions in the measurement area. These conditions provided both available fine sediments, which were re-mobilized at more exposed sites and transported in the water column as suspended matter, and suitable conditions for the deposition of fine sediments in the measurement area. In contrast, before and during TD2, the measurement area was exposed to wind waves, resulting in higher hydrodynamic loading of the sediment surface, which led to erosion of the upper sediment layers. Prior to campaign TD4, trends in the wind conditions were less distinct.

4.2. Erosion experiments

4.2.1. Temporal variability of the erosion process and erosion threshold

Erosion experiments have been conducted during the four measuring campaigns (TD1 to TD4) in-situ and ex-situ in the field and in the laboratory. The in-situ experiments are expected to provide conditions closest to nature, hence the in-situ experiments of each campaign are compared in this section to investigate the temporal variation of the erosion process and specifically the erosion threshold over the period of several months. Fig. 6 shows an overview of the conducted in-situ experiments of the campaigns TD1, TD2 and TD4. The in-situ experiment during TD3 exhibited comparable erosion behavior as the TD1 experiments (see Fig. 7 for full overview).

Fig. 6A–C shows the stepwise increase in applied bed shear stress over time, along with the corresponding evolution of suspended sediment concentration (SSC) measured in the C-GEMS. The resulting erosion rates (ε) are presented in Fig. 6D–F. In the TD1 experiments, a notable increase in SSC and consequently ε was observed around 120 min into the experiment. In contrast, for TD2 and TD4, this increase occurred much earlier, after 20–45 min and 45–60 min, respectively. For all experiments, SSC continued to rise with each subsequent load step. Following the onset of floc erosion, erosion rates in TD1 and TD2 increased sharply, reaching values up to 4 x 10^{-4} kg/(m^2s), and remained within this range until the experiment concluded. In TD4, however, both the maximum erosion rates were slightly lower and the increase in ε was more gradual. These patterns are mirrored in the SSC profiles. Each new load step, marked by an increase in bed shear stress, typically results in a peak in erosion rate, followed by a gradual decline

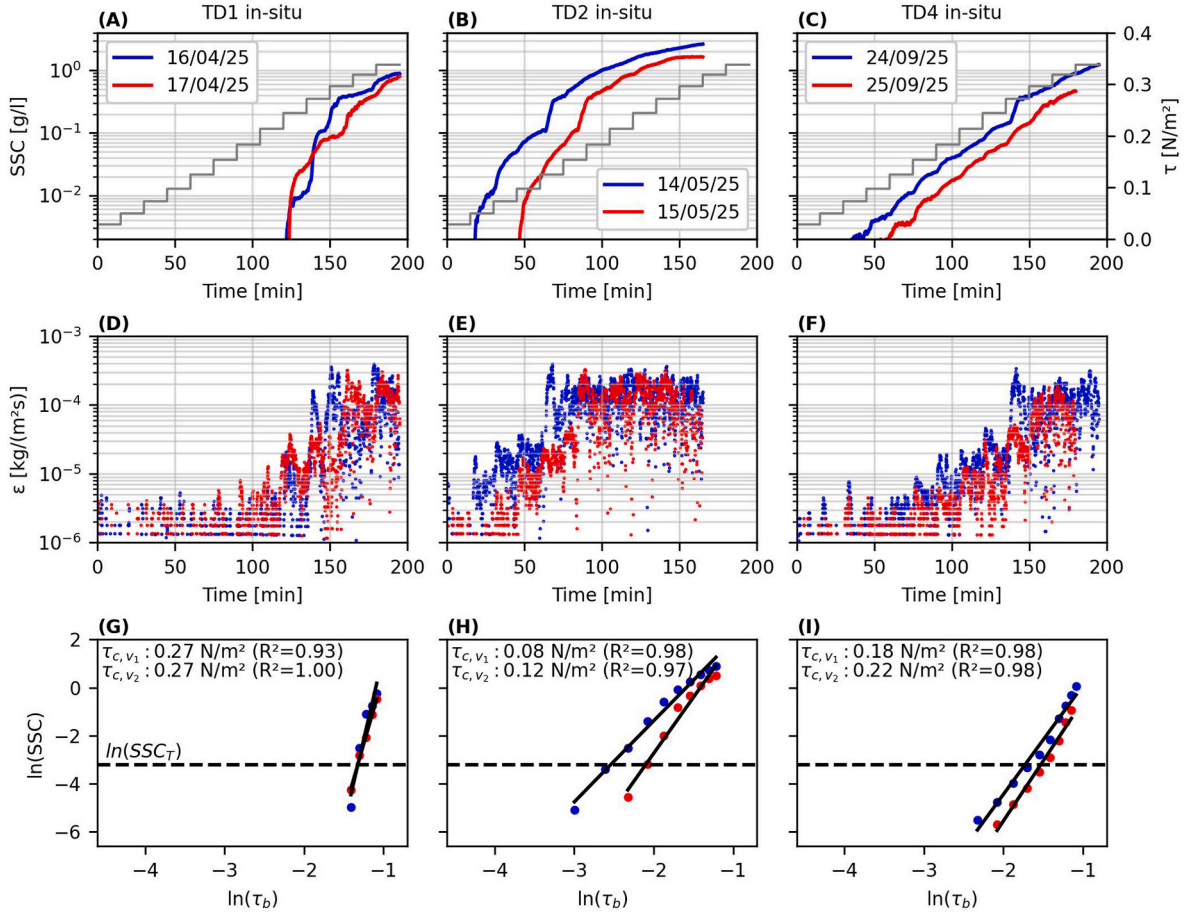

Fig. 6. Comparison of in-situ erosion experiments of campaigns TD1, TD2 and TD4. Panels A–C show the respective evolution of the measured SSC over the experimental duration. Panels D–F display the derived erosion rates ε. Panels G–I illustrate the log-log regressions of the load step averaged SSC. The intersection point of $\ln(SSC_T)$ and the regression line corresponds to $\ln(\tau_c)$.

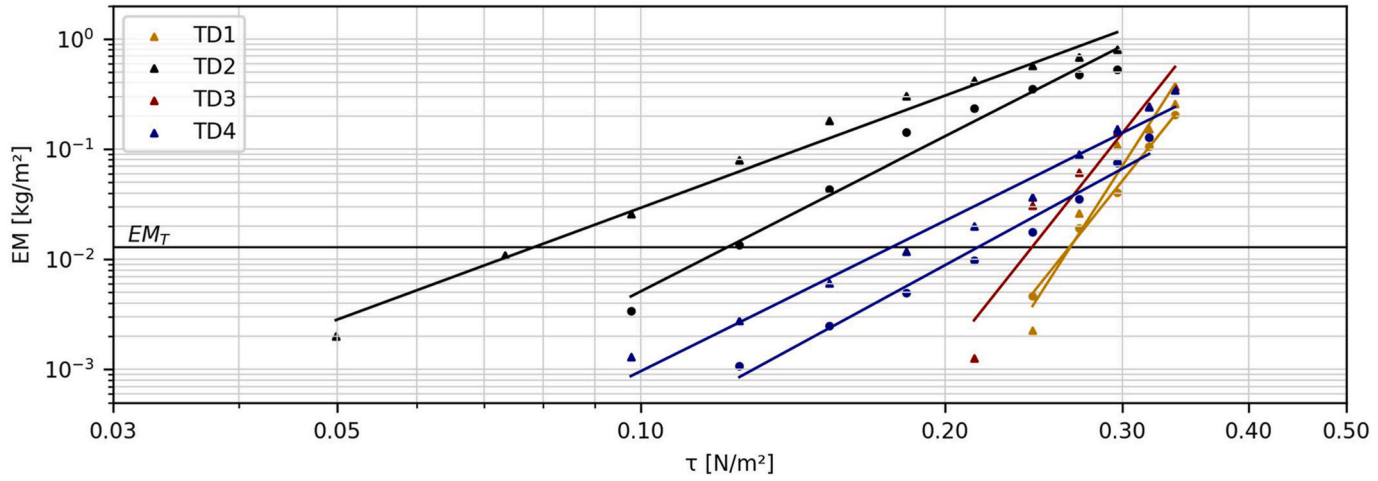

Fig. 7. Load step averaged total eroded mass (EM [kg/m^2]) for the in-situ experiments of the different measuring campaigns. The threshold value EM_T ~0.013 kg/m^2 is obtained by generalizing SSC_T by relating it to the C-GEMS fluid volume and the area of the test section.

over the duration of that load step. This behavior is commonly observed in erosion experiments involving cohesive sediments. It can be attributed to two factors: i) increasing erosion resistance with depth (erosion depth max. ~2 mm in the conducted experiments) and ii) the probabilistic nature of both the applied shear stress and the erosion resistance of individual sediment particles (Winterwerp et al., 2012).

To determine the critical erosion thresholds τ_c, a log-log regression of the mean SSC per load step against the applied bed shear stress τ_b was calculated and solved for SSC_T for each individual experiment (see section 3.1.2). The regression parameters, coefficients of determination (R^2), mean absolute errors (MAE), and resulting values of τ_c are summarized in Table 2. For TD1, both repetitions of the in-situ experiments yielded values for τ_c of 0.27 N/m^2. For TD2, τ_c ranged between 0.08 and 0.12 N/m^2 and for TD4, between 0.18 and 0.22 N/m^2. In the single TD3 experiment, where the SSC- and ε-evolutions were comparable to TD1, a τ_c value of 0.24 N/m^2 was determined. Fig. 6G–I illustrates the results of the log-log regressions. Fig. 7 provides an overview of all in-situ experiments, showing the load step-averaged total eroded mass (EM [kg/m^2]) plotted against the applied bed shear stress. Converting the SSC measured in the C-GEMS into EM – by relating it to the system's fluid volume and the area of the test section – allows for better comparison with results obtained using erosion devices of different sizes or types. In Fig. 7, the results are shown in the original data space, displayed on logarithmically scaled axes, to facilitate interpretation.

The repeated in-situ experiments conducted within a single measurement campaign showed a high degree of consistency, demonstrating the repeatability of both the experimental procedure and the results. The minor variations observed between repetitions within a measurement campaign were likely due to small-scale spatial heterogeneity of the mudflat. In contrast, the results from different measurement campaigns revealed significant variability, indicating temporal changes in both the erosion process and τ_c across campaigns (Figs. 6 and 7). Comparing the calculated mean erosion thresholds of the different campaigns with the respective sediment properties described in section 4.1, it is noticeable that the erosion thresholds for campaigns TD1, TD3 and TD4, for which the surface sediments had clearly cohesive character, were considerably higher than for campaign TD2, for which the surface sediments were rather weakly-cohesive to non-cohesive. This finding is in line with previous studies, which found a minimum τ_c for (homogeneous) sediments with particle sizes in the range of coarse silt and increasing values of τ_c for smaller particles, due to the increasing importance of interparticular bindings (cf. Grabowski et al. (2011)). Focusing on the campaigns with cohesive surface sediments, the highest values for τ_c were derived for TD1 and TD3, for which the surface sediments had slightly lower bulk densities, but higher mud contents compared to TD4. The accordance of these findings with the relations proposed by a recent mathematical model for the erosion threshold of cohesive sediments is investigated in section 4.2.3. No distinct influence of the biofilm, which was present at the sediment surface during campaigns TD3 and TD4, on the erosion characteristics was observed.

Houwing (1999) and Debnath and Chaudhuri (2010) provide comprehensive overviews of the τ_c values reported in earlier in-situ studies on mudflat erodibility. The values typically range from 0.03 to 0.74 N/m^2, placing the results of the present study well within this range.

Table 2
Regression parameters, coefficient of determination (R^2), mean absolute error (MAE) and resulting τ_c of the conducted in-situ experiments. R^2 and MAE refer to the log-transformed data.

Campaign	Date	Regression values ($ln(SSC) = m^*ln(\tau_b) + a$)				τ_c [N/m^2]
		m [-]	a [-]	R^2 [-]	MAE [-]	
TD1	16/04/25	14.29	15.69	0.93	0.410	0.27
	17/04/25	11.48	11.99	1.00	0.065	0.27
TD2	14/05/25	3.38	5.37	0.98	0.206	0.08
	15/05/25	4.67	6.60	0.97	0.239	0.12
TD3	27/08/25	–	–	–	–	–
	28/08/25	11.56	13.08	0.92	0.449	0.24
TD4	24/09/25	4.53	4.62	0.98	0.238	0.18
	25/09/25	4.99	4.42	0.98	0.205	0.22

4.2.2. Comparison of in-situ and ex-situ erosion experiments

In order to assess the influence of the extraction and transport of the sediment samples on the erosion threshold, erosion experiments with extracted sediment cores were carried out in the vicinity of the measurement area (ex-situ (field)) and in the laboratory (ex-situ (lab.)) in addition to the in-situ experiments. A detailed comparison of the results from campaign TD4 across the different types of erosion experiments is presented in Fig. 8. The evolutions of both SSC and ε show similar patterns for the two repetitions of the in-situ and ex-situ experiments, conducted both in the field and in the laboratory, taking into account the expected natural variability of the sediment samples. Nonetheless, for the ex-situ experiments a slight tendency to an earlier onset of (floc-) erosion and higher SSC values/erosion rates compared to the equivalent load step of the in-situ experiments could be observed. Thus, the derived mean erosion thresholds for the ex-situ experiments were lower than those for the in-situ experiments.

The results of the derived τ_c for all measuring campaigns and types of erosion experiments are summarized in Table 3 and visualized in Fig. 9. Except for TD2, the mean τ_c derived from the ex-situ experiments were

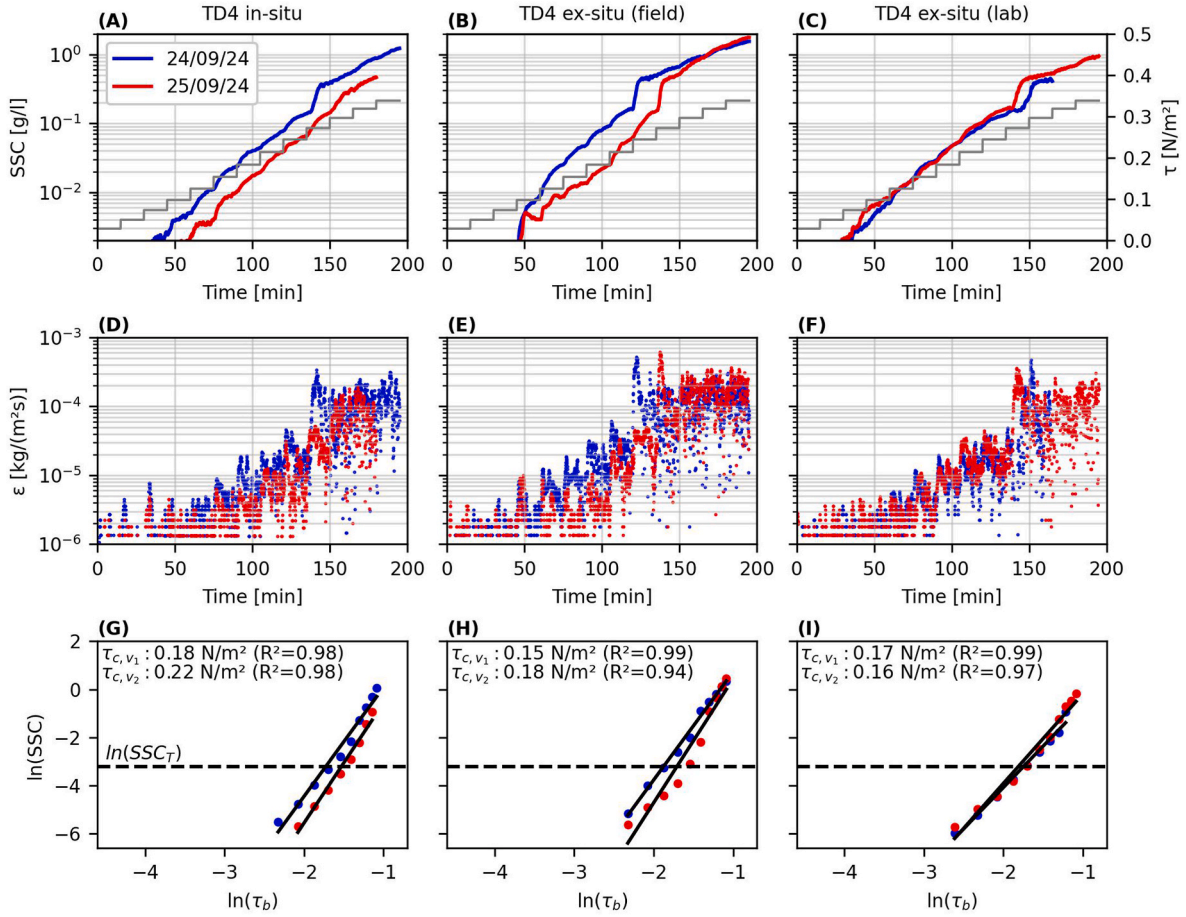

Fig. 8. Comparison of in-situ and ex-situ erosion experiments of campaign TD4. Panels A–C show the respective evolution of the measured SSC over the experimental duration. Panels D–F display the derived erosion rates ε. Panels G–I illustrate the log-log regressions of the load step averaged SSC. The intersection point of $\ln(SSC_T)$ and the regression line corresponds to $\ln(\tau_c)$.

Table 3
Overview of the derived erosion thresholds for all conducted measuring campaigns and types of erosion experiments. The relative change of the mean erosion threshold for the ex-situ experiments is calculated in relation to the mean value derived in the in-situ measurement (SR ≙ semi-range).

Campaign	In-situ	Ex-situ (field)		Ex-situ (lab.)	
	τ_c (±SR) [N/m^2]	τ_c (±SR) [N/m^2]	Rel. Change	τ_c (±SR) [N/m^2]	Rel. Change
TD1 (04/24)	0.27 ± 0.00	–	–	0.11 ± 0.01	−59.1 %
TD2 (05/24)	0.10 ± 0.02	0.10 ± 0.01	+0.5 %	0.10 ± 0.01	−0.5 %
TD3 (08/24)	0.24	0.22 ± 0.01	−11.0 %	0.19 ± 0.01	−21.1 %
TD4 (09/24)	0.20 ± 0.02	0.17 ± 0.01	−15.2 %	0.17 ± 0.01	−14.4 %

consistently lower than those derived from the in-situ experiments. For TD1, the difference in the derived mean τ_c between the in-situ and laboratory experiments was particularly high, with a decrease of τ_c of nearly 60 % in the laboratory experiments. As described in section 3.1.3, the samples collected for TD1 laboratory experiments were exposed to vibrations during the transport, due to the unsuitable tires of the handcart used for transportation on the Trischendamm. Presumably, the vibrations caused liquefaction of the cohesive surface sediment layer due to intrusion of the overlying water, reducing the erosion resistance of the samples. In response to these results, a handcart with vibration-damping tires was used for all subsequent campaigns and the execution of the ex-situ (field) experiments was initiated to differentiate between the influence of the extraction and the transport on the erosion threshold of the sediment samples. For the TD3 and TD4 experiments, in which the surface sediments were also cohesive, the reduction in τ_c in the ex-situ experiments (both field and lab.) compared to the in-situ measurements was ~10–20 %. For both campaigns, a reduction in τ_c of 10–15 % was already observed for the ex-situ (field) experiments. Thus, despite careful extraction and preparation of the sediment samples, minor disturbances of the surface sediments seemed to have occurred. The trend between ex-situ (field) and ex-situ (lab.) experiments of these campaigns was not distinct, with a further reduction in τ_c for TD3 and unchanging results for TD4. Compared to TD1, the reduction in τ_c measured in the laboratory experiments was significantly reduced due to the adapted transport of the samples for these campaigns. No reduction in the derived erosion threshold was observed for the ex-situ experiments conducted during TD2. Since the TD2 surface sediments were of rather non-cohesive character, their transport behavior was characterized not by bulk properties, but by the single sediment particles. Therefore, the surface layer and its erosion threshold were not, or only marginally, susceptible to intrusion by the water above.

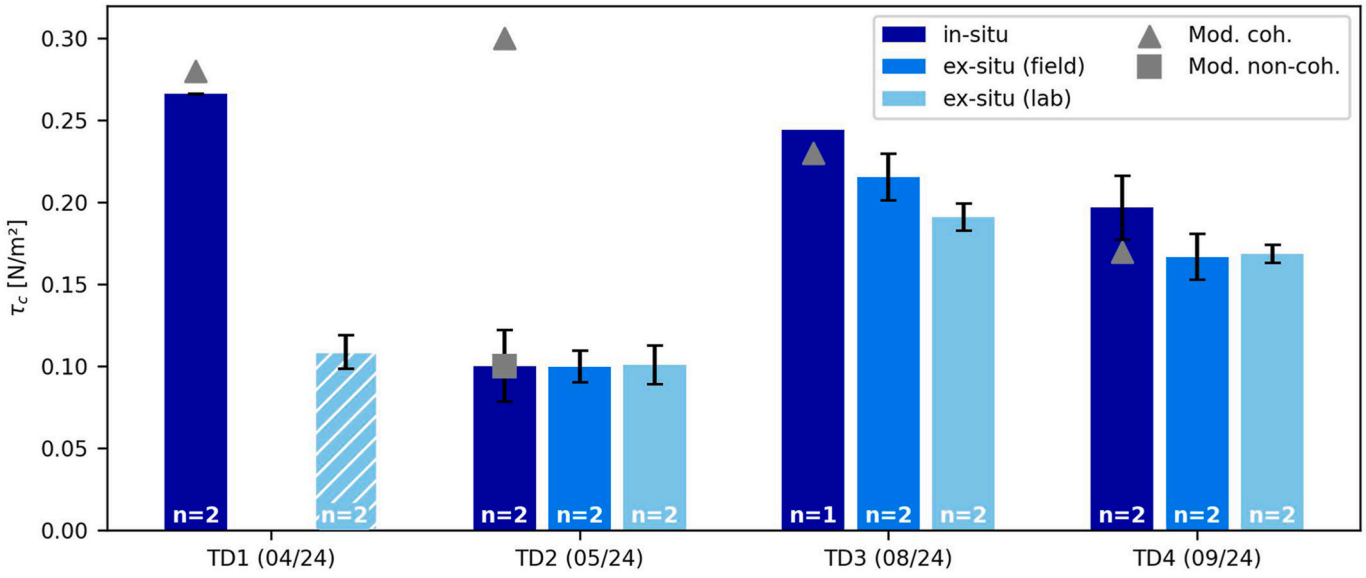

Fig. 9. Derived mean erosion thresholds for the four measuring campaigns and different types of erosion experiments. In case n > 1 (n ≙ number of repetitions), the error bar indicates the range of the conducted experiments. The samples collected for TD1 laboratory experiments were exposed to vibrations during transport.

The comparison of the in-situ and ex-situ erosion experiments of all conducted measuring campaigns suggests that the erosion threshold of cohesive sediments may be underestimated when derived from ex-situ experiments. Despite great care during sampling and transport, it appears that (non-visual) disturbances of the sediment samples could not be completely avoided. The level of reduction, in turn, may vary greatly, depending on details in the specific sampling or transport procedure. For future erosion experiments, careful consideration should be given to whether the tests should be carried out in-situ, despite the high effort involved, or whether an assessment of the erosion threshold in ex-situ experiments is sufficient. Further comparative experiments at the beginning of an investigation can also be useful in order to estimate the magnitude of the deviation between in-situ and ex-situ experiments. In general, conducting ex-situ experiments directly at the extraction site reduces the risk of further disturbances of the sediment samples during transport. The erosion characteristics of non-cohesive sediment samples appear to be less sensitive to sample extraction and transport and may therefore be investigated ex-situ.

4.2.3. *Modelling of the in-situ erosion thresholds*

This section investigates the agreement between the derived range and trends of in-situ erosion thresholds and the behavior predicted by the mathematical model recently proposed by Chen et al. (2021). The model is designed to be suitable for both cohesive and non-cohesive sediment mixtures and assumes that the erosion threshold increases with the dry bulk density of the mud component (clay and silt). The comprehensive formulation of the model is as follows (Eq. (2)):

$$\tau_c = \Theta_{cr,d_{s^*}} (\rho_{ps} - \rho_w) g d_s + A \frac{1}{d_{m,50}} (\rho_{dm}/\rho_{pm})^{\frac{2}{3}} \left[(\rho_{dm}/\rho_{pm})^{-\frac{1}{3}} - 1 \right]^{-2} exp(2.4\rho_{dm}/\rho_{pm}) \quad \text{Eq. 2}$$

Where the first term describes the erosion threshold of non-cohesive sediments with the Shields parameter Θ_{cr} (Shields, 1936). The parameter d_s is the dimensional particle diameter of the sand fraction, while ρ_{ps}, ρ_w and g describe the particle density of the sand particles, the water density and the gravitational accelaration, respectively. The second term of Eq. (2) describes the increase in τ_c due to cohesive particles, with $d_{m,50}$ as median particle size of the mud fraction and ρ_{pm}, ρ_{dm} as the density of the mud particles and the dry bulk density of the mud component. Parameter A is a site-specific calibration parameter and is typically on the order of 10^{-6}-10^{-5} J/m^2. ρ_{dm} is calculated from the dry bulk density ρ_{db} as $\rho_{dm} = \rho_{db} P_m / (1 - \rho_{db} P_s / \rho_{ps})$. Herein, P_m and P_s denote the mud and sand content of the sediment mixture. ρ_{db} in turn is calculated from the (wet) bulk density ρ_b as $\rho_{db} = \rho_p (\rho_b - \rho_w) / (\rho_p - \rho_w)$, with ρ_p as weighted particle density based on the mud/sand content. The Shields-parameter in the first term of Eq. (2) can be calculated after Soulsby and Whitehouse (1997), who applied a correction for fine-grained particles to the Shields curve (Eq. (3)):

$$\Theta_{cr}(d_{s^*}) = \frac{0.3}{1 + 1.2 d_{s^*}} + 0.055 (1 - exp(-0.020 d_{s^*})) \quad \text{Eq. 3}$$

The dimensionless particle diameter of the sand fraction is defined as $d_{s^*} = d_s \left((\rho_{ps}/\rho_w - 1) g / \upsilon^2 \right)^{1/3}$, with υ being the kinematic viscosity of water.

The parameters used to calculate τ_c according to Eq. (2), and the derived values, are summarized in Table 4 for all measuring campaigns. The particle size distribution and bulk density values used in the calculations were derived from the respective surface sediment layer (i.e., the topmost layer of each campaign in Fig. 5). While $d_{m,50}$ varied for the different measuring campaigns, the median particle size of the sand fraction was consistently ~100 μm. The particle densities are assumed as 2.65 g/cm^3 for sand particles and 2.575 g/cm^3 for mud particles (cf. Malcherek (2010)). The value of the fit-parameter A was determined as 9.2 x 10^{-6} J/m^2.

For campaigns TD1, TD3, and TD4, the calculated τ_c values closely match the erosion thresholds derived from the in-situ experiments, with deviations of only 0.01–0.03 N/m^2. However, for campaign TD2, the calculated τ_c (0.29 N/m^2) is considerably higher the erosion threshold observed in the in-situ experiments (0.10 N/m^2). This discrepancy is attributed to an overestimation of the increase in τ_c due to cohesion by the applied model for the TD2 surface sediment mixture (second term in Eq. (2)). The mud fraction of the TD2 surface sediments consisted solely of silt, with clay and fine silt fractions either absent or nearly absent. Since these finer fractions are critical to the cohesive behavior of a sediment mixture, the TD2 surface sediments likely behaved as non-cohesive material. Recalculating τ_c for TD2 following Shields (1936) and Soulsby and Whitehouse (1997), using the median particle size of $d_{50,TD2}$ = 58 μm (i.e., considering only the first term of Eq. (2), corresponding to a non-cohesive sediment mixture), results in τ_c = 0.10

Table 4
Parameters used for modeling of the erosion thresholds and comparison of calculated and measured τ_c values.

Campaign	In-situ experiments	Parameters for calculation of τ_c								Chen et al. (2021) (*Soulsby and Whitehouse (1997))
	τ_c (±SR)	P_m	ρ_b	$d_{m,50}$	d_s	ρ_{ps}	ρ_{pm}	ρ_w	A	τ_c (±SR)
	[N/m^2]	%	g/cm^3	µm	µm	g/cm^3	g/cm^3	g/cm^3	J/m^2	[N/m^2]
TD1 (04/24)	0.27 ± 0.00	76	1.23	13	100	2.65	2.575	1.018	9.2 x 10^{-6}	0.28
TD2 (05/24)	0.10 ± 0.02	55	1.46	31						0.29 0.10*
TD3 (08/24)	0.24	85	1.20	18						0.23
TD4 (09/24)	0.20 ± 0.02	48	1.32	38						0.17

N/m^2, which closely matches the erosion threshold determined in the in-situ experiments.

Overall, the variations and trends in τ_c measured in the in-situ experiments of the different measuring campaigns are well reproduced by the applied mathematical model. The results suggest that, for practical engineering tasks, estimating the erosion threshold and its changes based on sediment composition and concentration may yield realistic values. One limitation of the computed model results is the limited availability of in-situ measured data points. Furthermore, the transition between cohesive and non-cohesive sediment behavior may not be accurately captured, for example if the commonly made assumption of a constant clay-to-silt ratio within the mud fraction does not hold (van Ledden, 2003; Winterwerp et al., 2021). Although the model is capable of describing the variability of the erosion threshold based on sediment concentration and composition, future studies could benefit from considering parameters related to organic activity, such as chlorophyll-a content, given that several authors have reported a potential influence on the erodibility of cohesive sediments (Austen et al., 1999; Zhu et al., 2019).

With regard to the limitations and uncertainties of the overall investigation, the selection of sites for the in-situ tests and sampling should be mentioned. Despite considerable efforts to ensure the use of comparable and representative samples, the selection process inevitably involves a certain degree of subjectivity. Moreover, the findings should be validated for other tidal flats, particularly in more exposed areas, to better understand the spatial and temporal variability of surface sediment composition and its influence on erosion properties.

5. Conclusions and outlook

In the present study, a newly developed in-situ setup of the C-GEMS was utilized for erosion experiments in a tidal mudflat located in the mouth of the Elbe in the German Wadden Sea during four measuring campaigns between April and September 2024. The in-situ experiments were analyzed to assess the temporal variability of the surface erosion threshold τ_c. Additionally, the in-situ experiments were compared to the results of ex-situ erosion experiments (field and lab.) with extracted sediment cores from the same site, to evaluate the influence of the extraction and transport of sediment samples on the derived erosion threshold. The erosion experiments were accompanied by the characterization of the mudflat sediments in layers up to a depth of ~12 cm for each measuring campaign, regarding the water content, bulk density and particle size distribution. The following conclusions can be drawn from the results:

1) The developed in-situ setup of the C-GEMS is well-suited for erosion experiments in tidal mudflats. Its field of application includes both experiments with extracted sediment cores and placed sediment beds, enhancing the comparability between different types of erosion experiments.
2) The composition and concentration of mudflat surface sediments may show significant temporal variability. A cohesive surface layer was present during TD1, TD3, and TD4, but absent during TD2, where surface sediments were non- or weakly cohesive. Water content and bulk density of the top layer ranged from 95 to 280 % and 1200–1460 kg/m^3, respectively. The differences in surface sediment composition can be attributed to the wind conditions before and during the measurement campaigns, as these affect the hydrodynamic load on the sediment surface. Depending on wind speed and direction, this can lead to either erosion or deposition of fine sediments in the study area.
3) The erosion thresholds measured in the in-situ experiments varied in a range of 0.1–0.27 N/m^2. The lowest mean value of $\tau_c = 0.1$ N/m^2 was determined for TD2 with rather non-cohesive surface sediments. For TD1, TD3 and TD4 mean values of $\tau_c = 0.2$–0.27 N/m^2 were obtained. These findings are in line with theory, which predicts a minimum in τ_c for non-cohesive particles in the range of coarse silt and increasing erosion resistance for smaller particles due to cohesion.
4) The biofilm observed at the sediment surface during TD3 and TD4 had no clear influence on the derived erosion threshold. The variability in τ_c could be described reasonably well by the concentration and composition of the surface sediments, using the model of Chen et al. (2021). The results suggest that, for practical engineering applications, estimating the erosion threshold and its variability based on these parameters may yield realistic values.
5) For campaigns with a cohesive surface sediment layer, τ_c values derived from ex-situ experiments were consistently lower than those obtained from in-situ measurements. This discrepancy is attributed to (non-visible) disturbances of the surface sediments during sampling, as well as to liquefaction caused by vibrations during transport. The reduction in τ_c was approximately 60 % in the TD1 laboratory experiments and around 10–20 % in the ex-situ field and laboratory experiments of TD3 and TD4. The extent of this reduction appears to be strongly influenced by specific aspects of the experimental procedure, particularly the transport of the sediment samples.
6) The findings indicate that ex-situ erosion experiments for cohesive sediments may lead to an underestimation of the erosion threshold. In future studies, careful consideration should be given to whether erosion experiments are carried out in-situ or ex-situ, taking into account the effort involved and the reliability of the results.

Based on the results of this study, further investigations are planned on the temporal and spatial distribution of cohesive fine sediments, as well as on the variability of the erosion threshold, using the developed in-situ C-GEMS setup. The aim is to extend the investigations to tidal mudflats of different hydrodynamic exposure in order to better understand the sediment exchange processes between the estuary and adjacent tidal mudflats and to determine under which conditions the mudflats act as a sink or source of cohesive sediments. The erosion device and the methodology presented in this study can also be applied to address a wide range of additional research topics – such as biological effects on cohesive sediment erosion, seasonal variations in erodibility or estuary-specific differences in erosion behavior – and offer a feasible

approach to collecting reliable field data for the calibration and validation of numerical models.

CRediT authorship contribution statement

M. Witt: Writing – original draft. **J. Patzke:** Writing – review & editing. **E. Nehlsen:** Writing – review & editing. **P. Fröhle:** Writing – review & editing.

Funding

This study was conducted as part of the research project ELMOD - "Simulation and analysis of the hydrological and morphological development of the Tidal Elbe for the period from 2013 to 2018". The project on which this report is based is funded by the German Federal Ministry of Research, Technology and Space (BMFTR) under the funding code 03F0928A. The responsibility for the content of this publication lies with the authors.

Publishing fees supported by Hamburg University of Technology (TUHH).

The authors would like to thank both institutions for the support.

Declaration of competing interest

The authors declare that they have no known competing financial interests or personal relationships that could have appeared to influence the work reported in this paper.

Nomenclature

Symbol	Unit	Description
Latin		
A	J/m^2	Calibration parameter
a	–	Regression value
d_{50}	m	Median particle size
$d_{m,50}$	m	Median particle size of mud
d_s	m	Particle diameter of sand
d_{s*}	–	Dimensionless particle diameter of sand
EM	kg/m^2	Total eroded mass
g	m/s^2	Gravitational acceleration
H_s	m	Significant wave height
m	–	Regression value
N	1/s	Revolutions per second
N	–	Number of repetitions
P_m	%	Mud content
P_s	%	Sand content
Q	m^3/s	Pump rate
R^2	–	Coefficient of determination
SSC_T	kg/m^3	SSC-Threshold
W	%	Water content
Greek		
ε	$kg/(m^2s)$	Erosion rate
Θ_{cr}	–	Shields parameter
υ	m^2/s	Kinematic viscosity
τ_b	N/m^2	Applied bed shear stress
τ_c	N/m^2	Critical erosion threshold
ρ_b	kg/m^3	Bulk density
ρ_{db}	kg/m^3	Dry bulk density
ρ_{dm}	kg/m^3	Dry bulk density of mud
ρ_p	kg/m^3	Particle density
ρ_{pm}	kg/m^3	Particle density of mud
ρ_{ps}	kg/m^3	Particle density of sand
ρ_w	kg/m^3	Water density

Data availability

Data will be made available on request.

References

Aberle, J., Nikora, V., Walters, R., 2004. Effects of bed material properties on cohesive sediment erosion. Mar. Geol. 207 (1–4), 83–93. https://doi.org/10.1016/j.margeo.2004.03.012.

Amos, C.L., Feeney, T., Sutherland, T.F., Luternauer, J.L., 1997. The stability of fine-grained sediments from the fraser river Delta. Estuar. Coast Shelf Sci. 45 (4), 507–524. https://doi.org/10.1006/ecss.1996.0193.

Andersen, T.J., 2001. Seasonal variation in erodibility of two temperate, microtidal mudflats. In *estuarine, coastal and shelf science*, 53 (1), 1–12. https://doi.org/10.1006/ecss.2001.0790.

Andersen, T.J., Lanuru, M., van Bernem, C., Pejrup, M., Riethmueller, R., 2010. Erodibility of a mixed mudflat dominated by microphytobenthos and Cerastoderma edule, east Frisian Wadden Sea, Germany. Estuar. Coast Shelf Sci. 87 (2), 197–206. https://doi.org/10.1016/j.ecss.2009.10.014.

Austen, I., Andersen, T.J., Edelvang, K., 1999. The influence of benthic diatoms and invertebrates on the erodibility of an intertidal mudflat, the Danish Wadden Sea. Estuar. Coast Shelf Sci. 49 (1), 99–111. https://doi.org/10.1006/ecss.1998.0491.

BAW, 2024. Digital hydro-morphological twin of the trilateral Wadden Sea - TrilaWatt -. Bundesanstalt für Wasserbau (BAW). https://trilawatt.eu/en/data/data-products/. (Accessed 16 December 2024).

Beckers, F., 2021. Investigations on Functional Relationships Between Cohesive Sediment Erosion and Sediment Characteristics. Dissertation. Universität Stuttgart, Stuttgart. Institut für Wasser- und Umweltsystemmodellierung, checked on 9/1/2021.

Berlamont, J.E., Ockenden, M., Toorman, E.A., Winterwerp, J.C., 1993. The characterisation of cohesive sediment properties. Coast. Eng. 21, 105–128.

Briggs, K.B., Cartwright, G., Friedrichs, C.T., Shivarudruppa, S., 2015. Biogenic effects on cohesive sediment erodibility resulting from recurring seasonal hypoxia on the Louisiana shelf. Cont. Shelf Res. 93, 17–26. https://doi.org/10.1016/j.csr.2014.11.005.

Chen, D., Zheng, J., Zhang, C., Guan, D., Li, Y., Wang, Y., 2021. Critical shear stress for erosion of sand-mud mixtures and pure mud. Front. Mar. Sci. 8, 713039. https://doi.org/10.3389/fmars.2021.713039.

Colina Alonso, A., van Maren, D.S., Oost, A.P., Esselink, P., Lepper, R., Kösters, F., et al., 2024. A mud budget of the Wadden Sea and its implications for sediment management. Commun. Earth Environ. 5 (1). https://doi.org/10.1038/s43247-024-01315-9.

Debnath, K., Chaudhuri, S., 2010. Cohesive sediment erosion threshold: a review. ISH Journal of Hydraulic Engineering 16 (1), 36–56. https://doi.org/10.1080/09715010.2010.10514987.

Deutscher Wetterdienst, 2024. Wind data for station "büsum". Available online at: https://opendata.dwd.de/climate_environment/CDC/observations_germany/climate/10_minutes/wind/recent/. (Accessed 18 October 2024).

Dickhudt, P.J., Friedrichs, C.T., Sanford, L.P., 2011. Mud matrix solids fraction and bed erodibility in the York river Estuary, USA, and other muddy environments. Cont. Shelf Res. 31 (10), S3–S13. https://doi.org/10.1016/j.csr.2010.02.008.

DIN, 2017. Geotechnical Investigation and Testing - Laboratory Testing of Soil - Part 4: Determination of Particle Size Distribution. DIN-Normenausschuss Bauwesen, Berlin. https://doi.org/10.31030/2362539 (ISO 17892-4:2016); German version EN ISO 17892-4:2016.

DIN, 2022. Geotechnical Investigation and Testing - Laboratory Testing of Soil - Part 1: Determination of Water Content. DIN-Normenausschuss Bauwesen, Berlin. https://doi.org/10.31030/3364115 (ISO 17892-1:2014 + Amd 1:2022); German version EN ISO 17892-1:2014 + A1:2022.

DIN, 2023. Earthworks - Chemical Tests - Part 1: Determination of Loss on Ignition; German Version EN 17685-1:2023. DIN-normenausschuss Bauwesen. https://doi.org/10.31030/3412786. Berlin.

Grabowski, R.C., Droppo, I.G., Wharton, G., 2011. Erodibility of cohesive sediment: the importance of sediment properties. Earth Sci. Rev. 105 (3–4), 101–120. https://doi.org/10.1016/j.earscirev.2011.01.008.

Gust, G., 1989. Method of Generating precisely-defined Wall Shearing Stresses. Applied for by Hydro Data Inc., St. Petersburg. Florida on 10/11/1989. App. no. 419649. Patent no. US4973165.

Gust, G., Müller, V., 1997. Interfacial hydrodynamics and entrainment functions of currently used erosion devices. In: Cohesive Sediments, pp. 149–174.

Ha, H.J., Ha, H.K., 2021. Comparison of methods for determining erosion threshold of cohesive sediments using a microcosm system. Front. Mar. Sci. 8, 695845. https://doi.org/10.3389/fmars.2021.695845.

Houwing, E.-J., 1999. Determination of the critical erosion threshold of cohesive sediments on intertidal mudflats along the Dutch Wadden Sea Coast. Estuar. Coast Shelf Sci. 49 (4), 545–555. https://doi.org/10.1006/ecss.1999.0518.

Lee, S.-C., Mehta, A.J., 1994. Cohesive sediment erosion. US Army Corps of Engineers. Coastal and Oceanographic Engineering Department. University of Florida, Gainesville, Florida. Report DRP-94-6.

Lepper, R., 2023. A Contribution to Understanding the Recently Enhanced Coastal Siltation in the German Wadden Sea, vol. 25. Hamburg University of Technology (Hamburger Wasserbau-Schriften. https://doi.org/10.15480/882.8712.

Lorenzen, J.M., 1960. 25 Jahre Forschung im Dienst des Küstenschutzes. Kuste 8, 7–28. https://hdl.handle.net/20.500.11970/100721.

Lotze, H.K., Reise, K., Worm, B., van Beusekom, J., Busch, M., Ehlers, A., et al., 2005. Human transformations of the Wadden Sea ecosystem through time: a synthesis. Helgol. Mar. Res. 59 (1), 84–95. https://doi.org/10.1007/s10152-004-0209-z.

Malcherek, A., 2010. Zur Beschreibung der rheologischen Eigenschaften von Flüssigschlicken. Kuste 77, 135–178.

Mehta, A.J., McAnally, W.H., 2008. Fine-grained sediment transport. In: García, Marcelo H. (Ed.), Sedimentation Engineering. Processes, Measurements, Modeling, and Practice. Reston, Va: American Society of Civil Engineers (ASCE Manuals and Reports on Engineering Practice, No. 110), pp. 253–306.

Mitchener, H.J., Torfs, H., 1996. Erosion of mud/sand mixtures. Journal of Coastal Engineering (29), 1–25.

Noack, M., Gerbersdorf, S.U., Hillebrand, G., Wieprecht, S., 2015. Combining field and laboratory measurements to determine the erosion risk of cohesive sediments best. Water 7 (9), 5061–5077. https://doi.org/10.3390/w7095061.

Panagiotopoulos, I., Voulgaris, G., Collins, M.B., 1997. The influence of clay on the threshold of movement of fine sandy beds. Coast. Eng. 32 (1), 19–43. https://doi.org/10.1016/S0378-3839(97)00013-6.

Patzke, J., Nehlsen, E., Fröhle, P., Hesse, R.F., 2022. Spatial and temporal variability of bed exchange characteristics of fine sediments from the weser Estuary. Front. Earth Sci. 10, 916056. https://doi.org/10.3389/feart.2022.916056.

Perkey, D., Smith, J., Priestas, A., 2020. Erosion Thresholds and Rates for Sand-Mud Mixtures. US Army Corps of Engineers. https://doi.org/10.13140/RG.2.2.34625.58724. ERDC/CHL TR-20-13.

Seo, J.Y., Choi, S.M., Ha, H.K., Lee, K.E., 2020. Enhanced erodibility of deep-sea sediments by presence of calcium carbonate particles. Geo Mar. Lett. 40 (5), 559–571. https://doi.org/10.1007/s00367-020-00651-x.

Shields, A., 1936. Anwendung Der Ähnlichkeitsmechanik Und Der Turbulenzforschung Auf Die Geschiebebewegung. Technische Hochschule Berlin, Berlin. Preußische Versuchsanstalt für Wasserbau.

Sievers, J., Milbradt, P., Ihde, R., Valerius, J., Hagen, R., Plüß, A., 2021. An integrated marine data collection for the German bight – part 1: subaqueous geomorphology and surface sedimentology (1996–2016). Earth Syst. Sci. Data 13 (8), 4053–4065. https://doi.org/10.5194/essd-13-4053-2021.

Soulsby, R.L., Whitehouse, R.J.S., 1997. Threshold of sediment motion in coastal environments. In: Pacific Coasts and Ports '97: Proceedings of the 13th Australasian Coastal and Ocean Engineering Conference and the 6th Australasian Port and Harbour Conference, pp. 145–150.

Ternat, F., Boyer, P., Anselmet, F., Amielh, M., 2008. Erosion threshold of saturated natural cohesive sediments: modeling and experiments. Water Resour. Res. 44 (11), 2007WR006537. https://doi.org/10.1029/2007WR006537.

Tolhurst, T.J., Black, K.S., Paterson, D.M., Mitchener, H.J., Termaat, G.R., Shayler, S.A., 2000a. A comparison and measurement standardisation of four in situ devices for determining the erosion shear stress of intertidal sediments. Cont. Shelf Res. 20 (10–11), 1397–1418. https://doi.org/10.1016/S0278-4343(00)00029-7.

Tolhurst, T.J., Riethmüller, R., Paterson, D., 2000b. In situ versus laboratory analysis of sediment stability from intertidal mudflats. Cont. Shelf Res. 20 (10–11), 1317–1334. https://doi.org/10.1016/S0278-4343(00)00025-X.

van Ledden, M., 2003. Sand-Mud Segregation in Estuaries and Tidal Basins. Dissertation. Delft University of Technology, Delft.

van Rijn, L.C., 1993. Principles of Sediment Transport in Rivers, Estuaries and Coastal Seas, 1 volume. Aqua Publications, Utrecht.

Weilbeer, H., Winterscheid, A., Strotmann, T., Entelmann, I., Shaikh, S., Vaessen, B., 2021. Analyse Der Hydrologischen Und Morphologischen Entwicklung in Der Tideelbe Für Den Zeitraum Von 2013 Bis 2018. https://doi.org/10.18171/1.089104.

Whitehouse, R.J.S., Soulsby, R.L., Spearman, J., Roberts, W., Mitchener, H.J., 2000. Dynamics of Estuarine Muds. A Manual for Practical Applications. Telford, London.

Widdows, J., Brinsley, M.D., Salkeld, P.N., Lucas, C.H., 2000. Influence of biota on spatial and temporal variation in sediment erodability and material flux on a tidal flat (westerschelde, the Netherlands). Mar. Ecol. Prog. Ser. 194, 23–37. https://doi.org/10.3354/meps194023.

Widdows, J., Friend, P.L., Bale, A.J., Brinsley, M.D., Pope, N.D., Thompson, C., 2007. Inter-comparison between five devices for determining erodability of intertidal sediments. Cont. Shelf Res. 27 (8), 1174–1189. https://doi.org/10.1016/j.csr.2005.10.006.

Winterwerp, J.C., van Kessel, T., van Maren, D.S., van Prooijen, B.C., 2021. Fine Sediment in Open Water, vol. 55. WORLD SCIENTIFIC.

Winterwerp, J.C., van Kesteren, W., van Prooijen, B.C., Jacobs, W., 2012. A conceptual framework for shear flow-induced erosion of soft cohesive sediment beds. J. Geophys. Res. 117 (C10). https://doi.org/10.1029/2012JC008072 n/a-n/a.

Witt, M., Patzke, J., Nehlsen, E., Fröhle, P., 2024. Deriving erosion thresholds of freshly deposited cohesive sediments from the port of Hamburg using a closed microcosm system. Front. Mar. Sci. 11, 1386081. https://doi.org/10.3389/fmars.2024.1386081.

Work, P.A., Schoellhamer, D.H., 2018. Measurements of Erosion Potential Using Gust Chamber in Yolo Bypass near Sacramento, California. US Geological Survey, Reston, Virginia, 2018–1062.

WSV, 2024a. DEM (2022) of the outer and lower elbe. Wasserstraßen- und Schifffahrtsverwaltung des Bundes (WSV). www.kuestendaten.de. (Accessed 16 December 2024).

WSV, 2024b. Water level data of the gauge "Büsum". Wasserstraßen- und Schifffahrtsverwaltung des Bundes (WSV).

Zhu, Q., van Prooijen, B.C., Maan, D.C., Wang, Z.B., Yao, P., Daggers, T., Yang, S.L., 2019. The heterogeneity of mudflat erodibility. Geomorphology 345, 106834. https://doi.org/10.1016/j.geomorph.2019.106834.